



Published in final edited form as:

*Mol Psychiatry*. 2017 September ; 22(9): 1298–1305. doi:10.1038/mp.2016.258.

## Glutamate imaging (GluCEST) reveals lower brain GluCEST contrast in patients on the psychosis spectrum

David R. Roalf<sup>a</sup>, Ravi Prakash Reddy Nanga<sup>b</sup>, Petra E. Rupert<sup>a</sup>, Hari Hariharan<sup>b</sup>, Megan Quarmley<sup>a</sup>, Monica E. Calkins<sup>a</sup>, Erich Dress<sup>a</sup>, Karthik Prabhakaran<sup>a</sup>, Mark A. Elliott<sup>b</sup>, Paul J. Moberg<sup>a</sup>, Ruben C. Gur<sup>a</sup>, Raquel E. Gur<sup>a</sup>, Ravinder Reddy<sup>b</sup>, and Bruce I. Turetsky<sup>a</sup>

<sup>a</sup>Neuropsychiatry Section, Department of Psychiatry, University of Pennsylvania, Philadelphia PA 19104, USA

<sup>b</sup>Department of Radiology & Center for Magnetic and Optical Imaging, University of Pennsylvania Perelman School of Medicine, University of Pennsylvania, Philadelphia PA 19104, USA

### Abstract

Psychosis commonly develops in adolescence or early adulthood. Youths at clinical high risk (CHR) for psychosis exhibit similar, subtle symptoms to those with schizophrenia (SZ). Malfunctioning neurotransmitter systems, such as glutamate, are implicated in the disease progression of psychosis. Yet, *in vivo* imaging techniques for measuring glutamate across the cortex are limited. Here we use a novel 7 Tesla MRI glutamate imaging technique (GluCEST) to estimate changes in glutamate levels across cortical and subcortical regions in young healthy individuals and ones on the psychosis spectrum. Individuals on the psychosis spectrum (PS; n=19) and healthy young individuals (HC; n=17) underwent MRI imaging at 3T and 7T. At 7T, a single slice GluCEST technique was used to estimate *in vivo* glutamate. GluCEST contrast was compared within and across the subcortex, frontal, parietal and occipital lobes. Subcortical [ $\chi^2(1) = 4.65, p=0.031$ ] and lobular [ $\chi^2(1) = 5.17, p=0.023$ ] GluCEST contrast levels were lower in PS compared to HC. Abnormal GluCEST contrast levels were evident in both CHR (n=14) and SZ (n=5) subjects, and correlated differentially, across regions, with clinical symptoms. Our findings describe a pattern of abnormal brain neurochemistry early in the course of psychosis. Specifically, CHR and young SZ exhibit diffuse abnormalities in GluCEST contrast attributable to a major contribution from glutamate. We suggest that neurochemical profiles of GluCEST contrast across cortex and subcortex may be considered markers of early psychosis. GluCEST methodology thus shows promise to further elucidate the progression of the psychosis disease state.

### Keywords

Psychosis; glutamate; schizophrenia; clinical high risk; 7T MRI

---

Users may view, print, copy, and download text and data-mine the content in such documents, for the purposes of academic research, subject always to the full Conditions of use: [http://www.nature.com/authors/editorial\\_policies/license.html#terms](http://www.nature.com/authors/editorial_policies/license.html#terms)

Please address correspondence to: David R. Roalf, Ph.D., Department of Psychiatry, Neuropsychiatry Section, Brain Behavior Laboratory, 10<sup>th</sup> Floor, Gates Building, Hospital of the University of Pennsylvania, Philadelphia, PA 19104, [roalf@upenn.edu](mailto:roalf@upenn.edu).

**CONFLICT OF INTERESTS:** The authors declare no competing financial interests.

## Introduction

Psychosis is a complex brain disorder that often develops in late adolescence.<sup>1–3</sup> There is strong evidence that cortical microcircuitry is abnormal in psychosis. Patients with psychosis, specifically schizophrenia (SZ), exhibit progressive brain tissue loss<sup>4, 5</sup>, reduced cortical neuropil<sup>6</sup>, altered dopaminergic modulation<sup>7, 8</sup>, and abnormal excitatory and inhibitory neurotransmitter functioning<sup>9–13</sup>. Such deficits are also found, to a lesser extent, in youths at risk for developing psychosis.<sup>14–16</sup> These at-risk youths exhibit attenuated psychotic symptoms which evolve into frank psychosis about 35% of the time.<sup>17,18</sup> Recent evidence indicates that dysregulation of the dopamine system in psychosis may be secondary to deficits in glutamate (e.g. NMDA receptor) function<sup>8</sup>, hence measurement of brain glutamate may provide a sensitive marker early in the disease course and in those at risk for psychosis.

Proton magnetic resonance spectroscopy (<sup>1</sup>H MRS) can identify abnormal neuronal integrity at the molecular level.<sup>8</sup> Changes in glutamatergic metabolites including glutamate (Glu), glutamine (Gln) and the combination of glutamate and glutamine (Glx) appear related to the course of SZ. However, findings are not consistent. As documented in a recent meta-analysis<sup>19</sup>, glutamatergic metabolites are, on average, higher in clinical cases compared to controls. But the presence and magnitude of any elevation depends upon patient subgroup (chronic schizophrenia, high risk individuals or first episode patients), particular brain region and medication status. As an illustration, first-episode patients show higher glutamate in the striatum and cerebellum during an antipsychotic-naïve condition as compared to controls; yet glutamate levels were equivalent after patients received 4 weeks of antipsychotic medication.<sup>20</sup> Other studies have reported lower glutamate in medicated patients,<sup>21,22</sup> and this was true for both younger and older patients,<sup>22</sup> further suggesting that antipsychotic medications may lower glutamate/glutamine levels. In contrast, young never-treated SZ patients show *higher* glutamate levels in medial prefrontal cortex<sup>21</sup> and higher glutamine in the anterior cingulate and thalamus<sup>23</sup>, although several studies report the opposite or null effects within many of these regions (see<sup>8</sup> for review). Finally, postmortem studies corroborate glutamate system dysfunction in patients with schizophrenia through reports of altered glutamate receptor binding, transcription and protein expression in schizophrenia.<sup>24–26</sup>

MRS findings in clinical high risk (CHR) are even less consistent.<sup>19, 27</sup> Meta-analytic results indicate that CHR individuals show elevated Glx only within the medial frontal cortex<sup>19</sup>, whereas specific studies indicate lower,<sup>15, 16, 28–30</sup> higher<sup>29–35</sup> and no difference<sup>36–38</sup> in glutamate (or glutamate/glutamine) in several brain regions in an assortment of CHR cohorts, including clinically and genetically high risk samples followed longitudinally. In addition, several studies indicate that glutamate levels, particularly in the striatum, are associated with the transition to psychosis<sup>15, 16, 28, 33</sup>. In CHR, lower thalamic glutamate levels are both positively and negatively associated with gray matter volume in regions across the cortex<sup>29</sup>, many of which are critical in the pathogenesis of psychosis. Furthermore, CHR individuals show hypermetabolism, as measured by cerebral blood volume, in the hippocampus<sup>39</sup> that is associated with gray matter volume loss, predicts conversion to psychosis and corresponds with animal models suggesting excess extracellular

glutamate may regulate volume loss. Thus, the role and time course of glutamate changes, particularly early in the course of psychosis, remain unclear.

*In vivo* measurement of neurotransmitter levels can provide insight into the functional role of brain structures. However, quantification of neurotransmitters across the cerebrum is limited with spectroscopic techniques. Recently, we implemented a novel MRI method for measuring brain glutamate (Glu) in human cortex,<sup>40, 41</sup> based on glutamate chemical exchange saturation transfer (GluCEST). Briefly, CEST measures brain metabolites/macromolecules with exchangeable protons (-OH, -NH<sub>2</sub>, -NH).<sup>42-46</sup> When magnetization from the exchangeable protons of a metabolite (e.g., glutamate) is saturated with a frequency-selective radiofrequency pulse (in this case tuned for amine group protons), a proportional decrease of the water signal results from the exchange mediated accumulation of saturated protons in the bulk water pool. The difference between these two water signals obtained with and without saturation of the metabolite pool is measured as the CEST effect. Thus, the change in free water magnetization, while selectively saturating the exchangeable protons of the metabolite, represents a measure of the metabolite content. GluCEST has higher sensitivity than traditional <sup>1</sup>H MRS for measuring glutamate<sup>40</sup> and animal models indicate that GluCEST contrast has a major contribution (>70%) from glutamate<sup>40</sup>. While the combined contribution from other amines, amides, and creatine can be as high as 30%<sup>40</sup>, contribution from glutamine is low.<sup>40</sup> GluCEST has been used to estimate changes in glutamate in mouse models of Alzheimer's disease<sup>47, 48</sup> and Huntington's disease<sup>49</sup> and in the brain<sup>41</sup> and spinal cord of healthy subjects<sup>42</sup>, and clinically in epileptic patients<sup>50</sup>. As reviewed by Poels et al.<sup>8</sup> in SZ and Treen et al.<sup>27</sup> in CHR, there is evidence that glutamate levels are disrupted in early-stage drug-free patients with SZ and in CHR individuals. Yet, these findings are inconsistent and have significant limitations, including study heterogeneity, potential confounding effects of antipsychotic medication, different field strengths and the use of single voxel spectroscopy over different brain regions. While the GluCEST method and our current approach do not overcome all of these limitations, GluCEST offers specific advantages including: 1) higher sensitivity than MRS, 2) the ability to assess glutamate unconfounded by glutamine, and 3) better spatial resolution, as measurement of brain glutamate is feasible across many brain regions.

The goal of the current study was to measure GluCEST contrast levels in individuals on the psychosis spectrum (SZ+CHR) and healthy controls (HC) at 7T using the novel single slice GluCEST approach that will capture changes in brain metabolites across the cortex. We hypothesized that SZ+CHR would show regionally specific alterations in GluCEST contrast as compared to HC.

## Materials and methods

### Participants

Psychosis spectrum (PS) participants (n=21) included both young individuals at high clinical risk for psychosis and recently diagnosed schizophrenia patients (Table 1). CHR (n=15), SZ (n=5) and HC (n=21) subjects all received comprehensive clinical assessments, including a structured diagnostic interview to assess a broad spectrum of psychosis-relevant experiences. Assessment instruments included, as appropriate, a modified version of the Schedule for

Affective Disorders and Schizophrenia for School Age Children – Present and Lifetime Version (K-SADS-PL)<sup>51</sup>, the Structured Clinical Interview for DSM-IV-TR Axis I Disorders, Patient or Non-Patient Edition (SCID-I)<sup>52</sup>, and the Structured Interview for Prodromal Syndromes (SIPS)<sup>53</sup>. Rating scales included the Brief Psychiatric Rating Scale (BPRS)<sup>54</sup>, the Scales for Assessment of Negative Symptoms (SANS)<sup>55</sup> and Positive Symptoms (SAPS)<sup>56</sup>, and the Scale of Prodromal Symptoms (SOPS)<sup>57</sup>. Best estimate consensus diagnoses were assigned following case review by at least two doctoral level clinicians.

Subjects were classified as CHR if they had at least one positive OR two negative and/or disorganized symptoms rated 3, 4, or 5 on the SOPS, without meeting criteria for a DSM-IV Axis I psychotic disorder. SZ patients met DSM-IV criteria for schizophrenia and were within five years of their age of onset, defined as unambiguous evidence of overt psychotic symptoms associated with functional deterioration. HC individuals had no DSM-IV Axis I psychotic disorder, no super-threshold prodromal symptomatology, no history of psychosis in a first-degree biological relative, and no personal Axis II Cluster A diagnosis. One CHR reported current smoking, but no HC or SZ were ever smokers. Exclusion criteria are documented in Supplement Methods. All subjects provided informed consent or, for minors, informed assent and parental consent. The Institutional Review Boards of the University of Pennsylvania and The Children's Hospital of Philadelphia approved all procedures.

### 3T and 7T Structural MRI acquisition and region of interest selection

An optimized within-subject acquisition and analysis pipeline was implemented (Figure 1A). This procedure is documented in full in the Supplemental Methods. Briefly, participants underwent both 3T and 7T structural scanning to optimize 7T GluCEST acquisition. FreeSurfer version 5.3 was used to parcellate the 3T MRI and the Imscribe (cmroi.med.upenn.edu/imscribe) tool was used to localize the 3T region-of-interest to the 7T MRI, which enabled comparable field-of-view placement for GluCEST acquisition across subjects.

### GluCEST acquisition and analysis

The GluCEST imaging parameters were: slice number = 1, slice thickness = 5 mm, FOV: 220 × 200, Matrix size: 192 × 192, in-plane resolution = 1.15×1.15mm<sup>2</sup>, GRE read out TR = 6.2 ms, TE = 3 ms, number of averages = 1, shot TR = 10500 ms, shots per slice = 2, with a CEST saturation pulse at a  $B_{1rms}$  of 3.06  $\mu$ T with 500 ms duration. Raw CEST images were acquired at varying saturation offset frequencies from  $\pm 1.5$  to  $\pm 4.5$  ppm (relative to water resonance) with a step size of  $\pm 0.3$  ppm. The equation for calculating GluCEST contrast is: GluCEST contrast (%) = [(Msat(-3ppm) – Msat(+3ppm))/Msat(-3ppm)]\*100. GRE images at two echo times (TE1 = 4.24 ms; TE2 = 5.26 ms) were collected to compute  $B_0$  map.  $B_1$  map was generated from the two images obtained using square preparation pulses with flip angles 30° and 60°. Acquisition, time of CEST images,  $B_1$  and  $B_0$  field maps was approximately 12 minutes.  $B_0$  and  $B_1$  inhomogeneity effects in GluCEST maps were corrected using previously reported methods<sup>40</sup>. Additionally, voxels with  $B_0$  offset >1ppm and relative  $B_1$  values <0.3 or >1.3 were excluded in the GluCEST map calculation.

Example GluCEST maps are shown in Supplemental Figure 1. The final sample therefore included 19 PS (CHR=14; SZ=5) and 18 HC individuals.

Within the acquisition slab, GluCEST measurements were reported from the whole slice cortical gray matter and, separately, from the subcortex, frontal, parietal and occipital lobes (Figure 2B & 3A); overlap of each ROI across the single slice acquisition is reported in Table 2. Lobar volumes were estimated and are shown in Supplemental Figure 3.

## Statistical Analyses

Demographic and clinical group differences were examined with t-tests or chi-square tests. Differences in GluCEST contrast were assessed using the Generalized Linear Latent and Mixed Models (GLLAMM) algorithm implemented in Stata 14.1 (StataCorp; College Station, TX, USA), with group, sex, age, and lobe or region-of-interest as fixed-effects predictors of GluCEST contrast and subject as a random effect. The mixed model allowed all subject data to be included in the analysis, even though some subjects were missing data for one or more ROIs. The significance levels of individual model parameters were assessed using the Wald statistic with  $\chi^2$  distribution. Significant main effects and interactions were parsed by post-hoc computation of appropriate linear combinations of the model coefficients, along with their associated z-statistic and p-value. While the sample size in the current study is small, it was deemed adequate given the typical sample size in previous MRS studies and the higher sensitivity of GluCEST. Given the small SZ sample, patients were not analyzed as a separate group. Rather, initial analyses compared all PS subjects (SZ+CHR) with HC. Analyses with significant PS-HC differences were then repeated after excluding SZ subjects, to determine if observed deficits were unambiguously evident in CHR subjects prior to illness onset. The relationships between GluCEST contrast and clinical or demographic measures were examined using Pearson correlations, separately within each sample. Statistical significance threshold of  $p < 0.05$  was set for all analyses.

## Results

### Participant Characteristics

PS and HC groups did not differ in age, level of education, maternal education, sex or race distribution (Table 1).

### GluCEST in Psychosis Spectrum

**Cortical Gray Matter GluCEST**—There were no significant effects of group [ $\chi^2(1) = 2.84, p=0.092$ ], gender [ $\chi^2(1) = 0.71, p=0.40$ ], or age [ $\chi^2(1) = 0.01, p=0.91$ ], based on the entire brain tissue included in the GluCEST acquisition slab, although a clear trend was observed for group, with lower values in PS.

**Lobar GluCEST Measures**—Mean cerebral GluCEST contrast was lower, across the three lobes of the cortex, in PS compared to HC [ $\chi^2(1) = 5.17, p=0.023$ ]. There was also a significant effect of lobe [ $\chi^2(2) = 44.46, p < 0.0001$ ], with lower values apparent in the frontal lobe, but no interaction between lobe and group [ $\chi^2(1) = 0.56, p=0.75$ ; Figure 2]. There were no effects of age ( $p=0.79$ ) or gender ( $p=0.94$ ). The magnitude of the PS deficit

was ~16% in Frontal, ~14% in Parietal, and ~11% in Occipital lobes, compared to HC. A follow-up analysis contrasting just CHR to HC revealed virtually identical effects of group [ $\chi^2(1) = 4.82, p=0.028$ ] and lobe [ $\chi^2(2) = 41.27, p<0.0001$ ]. Again, there was no interaction between group and lobe, and no significant effects of age or gender. Across all subjects, GluCEST contrast was highly correlated across brain lobes: Frontal vs. Parietal  $r(36)=0.78, p<0.0001$ ; Frontal vs. Occipital  $r(34)=0.69, p<0.0001$ ; Parietal vs. Occipital  $r(34)=0.72, p<0.0001$ .

**Subcortex and Sublobar ROIs**—Subregional analyses revealed significant main effects of group and ROI within each lobe and the subcortex, but no interactions between group and subregion [PS vs. HC: Subcortex  $\chi^2(1) = 4.65, p=0.031$ ; Frontal  $\chi^2(1) = 7.55, p=0.006$ ; Parietal  $\chi^2(1) = 7.00, p=0.008$ ; Occipital [ $\chi^2(1) = 17.11, p<0.0001$ ]. Excluding SZ patients from the PS sample attenuated, but did not alter, any of these group effects [CHR vs. HC: Subcortex  $\chi^2(1)=4.45, p=0.035$ ; Frontal  $\chi^2(1) = 4.96, p=0.026$ ; Parietal  $\chi^2(1) = 5.37, p=0.020$ ; Occipital  $\chi^2(1) = 22.84, p<0.0001$ ] (Figure 3). Mean GluCEST contrast % is presented for each lobe and ROI, by group, in Table 2.

Gray matter volume deficits are commonly reported in PS<sup>58, 59</sup>, and volume was nominally, but not statistically lower in PS as compared to HC (Supplemental Results; Supplemental Figure 3). However, the findings reported above were not affected when volume was included as an additional covariate in analyses. White matter abnormalities are also common in PS<sup>60, 61</sup>, however neither white matter GluCEST nor volume differed between HC and PS. (Supplemental Figure 4).

**Exploratory Comparison of CHR and SZ**—As noted above, findings for the entire psychosis spectrum sample (CHR + SZ) and findings for the CHR sample alone, were virtually identical when compared to HC. Hence, these abnormalities are both present and relatively consistent prior to the onset of illness. We nevertheless considered, in an exploratory manner given the small SZ sample that subtler differences might exist between CHR and SZ. We therefore repeated all of the analyses, contrasting just CHR and SZ subjects. There were no differences for the brain slab [ $\chi^2(1) = 0.31, p=0.58$ ]. However, for the cortical lobar analysis within the CHR resulted in significant group [ $\chi^2(1) = 4.00, p=0.045$ ] and group X lobe [ $\chi^2(2) = 8.23, p<0.016$ ] effects. CHR had slightly *lower* GluCEST contrast overall, but also a different distribution profile across the three lobes. CHR subjects had GluCEST contrast measures that were lower than SZ in frontal and occipital cortex, but higher in parietal cortex (Figure 2).

For the subregional analyses within the subcortex we observed no overall difference between CHR and SZ [ $\chi^2(1) = 1.82, p=0.18$ ] and no interaction [ $\chi^2(3) = 2.75, p=0.43$ ]. In the frontal lobe, we observed no overall difference between CHR and SZ [ $\chi^2(1) = 1.95, p=0.16$ ], but a significant group X ROI interaction [ $\chi^2(4) = 10.67, p=0.030$ ]. CHR subjects were lower in the orbital frontal cortex and anterior cingulate, while SZ subjects were lower in the precentral cortex. Within the parietal lobe there were, again, no overall differences [ $\chi^2(1) = 0.81, p=0.37$ ], but a significant two-way interaction of group X ROI [ $\chi^2(4) = 14.41, p=0.006$ ], SZ patients had markedly lower measures in the superior parietal and postcentral cortices, regions in which CHR subjects were indistinguishable from healthy controls.

Finally, for the occipital lobe, there was an overall, significant CHR-SZ difference [ $\chi^2(1) = 4.15, p=0.041$ ] without an interaction effect [ $\chi^2(3) = 1.22, p=0.75$ ] (Figure 3).

**Association with clinical symptoms**—Correlations between symptoms and GluCEST contrast were estimated only within the PS sample. Summary clinical scores are shown in Table 1. As expected, PS individuals had higher positive and negative symptoms ratings than HC. SIPS positive [ $t(32)= 5.80, p<0.00001$ ], SAPS [ $t(32)= 4.64, p<0.0001$ ], SIPS negative [ $t(32)= 5.99, p<0.00001$ ], and SANS [ $t(32)= 4.52, p<0.0001$ ] scores were all higher in PS. Within the PS sample, higher positive symptoms, as indexed by SAPS, were associated with lower parietal GluCEST contrast [Pearson  $r(17) = -.49, p<0.05$ ]. Higher negative symptoms, as indexed by SANS, were associated with lower whole slice [Pearson  $r(17) = -.52, p<0.05$ ] and lower frontal lobe [Pearson  $r(17)=-0.52, p<0.05$ ] GluCEST contrast. However, these associations did not persist when SZ subjects were removed from the PS sample.

## Discussion

Using a novel imaging technique—glutamate chemical exchange saturation transfer—we identified abnormalities of neurochemistry in youth on the psychosis spectrum. GluCEST contrast levels were lower across subcortical and cortical brain regions in PS as compared to healthy young individuals. Abnormal GluCEST contrast levels were evident in youth at clinical high risk for psychosis and in a small sample of young patients with schizophrenia. Although deficits were evident across the brain, there were regionally specific associations with symptoms. Reduced GluCEST contrast in the frontal lobe correlated with negative symptoms, while contrast levels in the parietal lobe correlated with positive symptoms. To our knowledge this is the first report at 7 Tesla of lowered GluCEST contrast in the psychosis spectrum across the cerebrum.

Assuming changes in GluCEST contrast are due primarily to glutamate, these findings describe a pattern of abnormal brain neurochemistry early in the course of psychosis. At first glance our results appear at odds with several prior MRS studies (see Reviews<sup>8, 27</sup>), including the main finding of a recent comprehensive meta-analysis.<sup>19</sup> As documented in Merritt et al., 2016, glutamatergic metabolites are, on average, higher in “cases” — a designation that includes individuals with chronic schizophrenia, first episode patients and high-risk youth – as compared to controls. Yet, a careful examination of the region-specific effects within this meta-analysis reveals that when glutamate alone was reported (as opposed to glutamine or glutamate+glutamine), levels tended to be *lower* in cases compared to controls. Nominally lower glutamate levels were reported in medial prefrontal cortex, frontal white matter, medial temporal lobe, and thalamus, while glutamate levels were nominally elevated in the cerebellum and significantly elevated in *only* the basal ganglia (See Figure 1 in<sup>19</sup>). In contrast, when glutamine or glutamate+glutamine (Glx) levels were reported, cases showed consistently higher levels than controls. The strength of this elevation, however, was dependent upon both the specific patient subgroup (chronic schizophrenia, high risk individuals or first episode patients) and brain region. For example, meta-analytic results indicate that high-risk individuals have significantly higher Glx ( $d' = 0.26$ ) levels within the medial frontal cortex, but nominally lower glutamate levels within the same region. In fact, higher medial frontal Glx (as opposed to glutamate or glutamine) is the only meta-analytic

effect specific to high-risk individuals. This finding is noteworthy as it indicated elevated glutamate + glutamine, rather than glutamate alone. It is well documented that glutamate and glutamine MRS spectra are difficult to resolve at low field strengths and that glutamate MRS measures are likely to have some contribution from glutamine, albeit small<sup>62</sup>. Thus, while our observed effects may be contrary to prototypical MRS findings, those findings remain somewhat ambiguous. Importantly, the GluCEST contrast is relatively insensitive to glutamine as glutamine does not exhibit a CEST effect<sup>40</sup>. We therefore believe that GluCEST contrast offers an important new window into estimating brain glutamate that can be useful in understanding changes in the neurochemical profile in psychosis.

Our sample consisted predominantly of youth at risk for developing psychosis, thus our results are essentially reflective of this group. GluCEST contrast findings are consistent with some, but not all, recent spectroscopy findings in help-seeking CHR, which similarly suggested that CHR individuals have lower brain glutamate than healthy individuals<sup>15, 16</sup>. Initial reports using 3T MRI and single voxel approaches were less consistent, yet the findings still suggested that MRS measures of various brain metabolites may be sensitive to heightened psychosis risk or transition to psychosis<sup>28, 34, 63</sup>. Recent evidence indicates inter-individual differences in resting state glutamate (rsGlu) levels in the dorsal anterior cingulate – a region in which we also show significant deficits in CHR<sup>64</sup>. However, we acknowledge that our GluCEST contrast findings differ from meta-analytic MRS data indicating higher Glx levels within the medial frontal cortex in high-risk youth.<sup>19</sup> Yet, we believe that GluCEST contrast, even in a non-help seeking sample such as ours, may be a relevant marker of both functional impairment and incipient illness, potentially enhancing our ability to identify those individuals who are truly at risk for developing psychosis or otherwise have a poor functional prognosis. While we have few patients with psychosis in the current sample, our preliminary findings are consistent with some previous proton MRS studies.<sup>31, 65, 66</sup> Similar to our study, lower glutamate and glutamine levels were found within the anterior cingulate, albeit in the left hemisphere, in patients with SZ as compared to healthy volunteers<sup>67</sup> and progressively lower glutamate levels were found in frontal cortex in chronically ill SZ compared to HC<sup>9</sup>. However, in contrast to our findings, other MRS studies found never-treated young SZ had higher Glx levels in prefrontal cortex<sup>21</sup> and higher Gln in anterior cingulate and left thalamus<sup>23</sup>. These discrepancies are likely due to the insensitivity of GluCEST to glutamine. While initial GluCEST work<sup>40, 41</sup> indicates a high correspondence between MRS and GluCEST, a thorough within-subjects comparison of techniques in a larger sample will help clarify this issue.

Overall, lower GluCEST contrast across the cortex may reflect dysfunctional neurotransmission or downregulation of glutamatergic synapses in psychosis<sup>68</sup>. This may be the result of subtle, but widespread cortical atrophy known to exist in schizophrenia<sup>5, 69–72</sup> and clinical high risk<sup>58</sup>. Psychosis spectrum individuals in the current sample had nominally lower gray matter volumes, yet, there was no direct evidence that lower volume in PS was mediating lower GluCEST findings. Critically, this suggests that neurochemical changes are occurring prior to significant volumetric loss.

One proposed model of glutamate dysfunction in psychosis<sup>73</sup> posits that the loss of inhibitory control in PFC due to NMDA-mediated interneuron dysfunction leads to elevated

glutamate levels, which in turn, leads to an excitotoxic environment and eventual loss of glutamatergic receptors. Given this model, we might expect that cortical glutamate—and thus GluCEST contrast—would be diffusely elevated as several other studies report, rather than reduced, early in the course of illness. The fact that we find consistent reductions across all brain regions, in both prodromal and early psychosis suggests that the sequelae of glutamatergic dysfunction are already well under way in the early stages of the disorder. However, we cannot rule out the possibility that the etiological mechanisms that give rise to reduced GluCEST contrast in CHR and SZ subjects are not the same.

The finding of distinct, regionally specific associations of GluCEST contrast reductions in the frontal and parietal lobes with negative and positive symptoms, respectively, is an intriguing one. The idea that negative symptoms arise as a consequence of functional hypofrontality is a longstanding one that has received substantial prior empirical support<sup>74</sup>. Our data linking these symptoms directly to reduced GluCEST contrast in the frontal lobe offers a validation of this etiological model. However, the relationship between parietal lobe dysfunction and positive symptoms was unanticipated. Positive symptoms are usually thought of as manifestations of medial temporal lobe limbic system dysfunction<sup>75</sup> or, in the case of auditory hallucinations, abnormal activity in auditory cortex<sup>76</sup>. We note, though, recent reports on the effects of ketamine administration, which serves as a pharmacological model of glutamatergic NMDA dysfunction in schizophrenia<sup>77, 78</sup>. In these studies of healthy subjects, ketamine altered the fMRI BOLD response diffusely<sup>77</sup> and elevated anterior cingulate (ACC) glutamate<sup>78</sup>. However, symptomatic increases in positive symptoms were associated exclusively with changes in the BOLD signal of parietal lobe regions around the paracentral lobule<sup>77</sup> and with elevations of ACC glutamate<sup>78</sup>. Our data are consistent with the suggestion that the parietal lobe plays an important role in the manifestation of positive symptoms. Given the relationship we found between negative symptoms and GluCEST contrast, additional inquiries into drugs that modulate glutamatergic neurotransmission may yield novel, and possibility individualized treatments for both negative and positive symptoms associated with schizophrenia and youth at risk for this disorder. Characterization of these abnormalities in more detail in SZ is needed to shed light on potential targets of glutamate-modulating treatment strategies.

Previous work has detailed the advantages and limitation of the GluCEST technique<sup>41, 50</sup>. Direct conversion and comparison of GluCEST contrast to MRS quantities is challenging, and this may explain some of the discrepancies between previous MRS findings and our GluCEST results. GluCEST detects glutamate contrast through magnetization transfer between  $-NH_2$  protons and free water. Factors such as magnetic transfer asymmetry and minor contributions from creatine, GABA and other macromolecules<sup>40</sup> can affect GluCEST contrast. Importantly, about 70% of the observed CEST signal is from glutamate, with the remaining 30% coming from other exchangeable protons (though, notably, very little from glutamine). Despite this contamination, the GluCEST method can be used to study relative changes in glutamate and, in this regard, it is comparable to MRS measures.<sup>41, 49</sup> While MRS quantification is more direct, even short-echo MRS still includes signal from other macromolecules. In addition, GluCEST has a sensitivity advantage over MRS for glutamate, which leads to significantly improved signal with better spatial distribution, improving visualization of the functional excitatory system. Moreover, information can be acquired in

the same amount of time as conventional MRS. More systematic comparisons of these two approaches at 7T are clearly needed to establish both convergence and disparities. While we implement a gray matter parcellation and use this to localize ROI, it is likely that partial volume effects exist within our GluCEST contrast measure. Unlike typical single-voxel MRS we are able to separate GluCEST contrast signal from major white matter tracts post-hoc (see Supplemental Data), which we believe is a particular advantage of the GluCEST approach. We also note that PS individuals had nominally lower gray matter volume, which may increase saturation effects and subsequently the GluCEST effect, but it is unclear if these subtle changes in volume explain lower GluCEST in PS individuals. Given technological limitations at the outset of this study, GluCEST data were only acquired in a 5mm single slice. This limited our ability to analyze certain ROIs, due to equivocal coverage during acquisition and our ability to compare GluCEST results with the most robust MRS finding in the basal ganglia, medial temporal lobe, and thalamus<sup>19</sup>. However, 3D acquisition techniques will eliminate this concern going forward. GluCEST is specific to glutamate, which can be considered a limitation when attempting to compare GluCEST results with MRS data, where Glx and Gln are directly measurable. We note that 3 of the 5 patients with schizophrenia were on antipsychotic medications that could lower glutamate levels in our results. However, we find similar deficits in CHR youth who are not medicated and other studies report significantly lower glutamate in never treated schizophrenia patients<sup>23</sup>, thus reducing the likelihood that these effects are medication related. Finally, our sample size is relatively small, yet this is the largest study using 7T GluCEST in a patient population. We believe that this exciting new technique enables more comprehensive assessment of glutamatergic metabolites, particularly given the overlap of resonance frequencies of glutamate and glutamine at lower field strengths.

Our preliminary work indicates that youth at clinical high risk and young patients with schizophrenia exhibit significant abnormalities in GluCEST contrast across the cerebrum. We suggest that, in addition to other metrics, neurochemical profiles of glutamate across the cerebrum should be considered as markers of risk of developing a psychotic disorder. The use of 7T GluCEST shows promise to further elucidate the progression of psychosis, may provide a method for detecting neuropsychiatric disorders and could enhance pharmacological targeting.

## Supplementary Material

Refer to Web version on PubMed Central for supplementary material.

## Acknowledgments

Thanks to the acquisition and recruitment team: Jacqueline Meeks, Jeff Valdez, Elliott Yodh, R. Sean Gallagher, Jason Blake, Prayosha Villa, & Kevin Seelaus.

**FUNDING SOURCES:** This work was supported by National Institute of Mental Health R01MH099156 to BIT, K01MH102609 to DRR, P41 NIBIB EB015893 & R01 NINDS NS087516 to RR, and RC2 MH089983, P50 MH096891 & T32 MH019112 to REG. Additional support was provided by the Dowshen Program for Neuroscience at the University of Pennsylvania. The funding sources were not directly involved in study design, collection, data analysis or interpretation, nor manuscript writing.

## References

1. Casey BJ, Oliveri ME, Insel T. A neurodevelopmental perspective on the research domain criteria (RDoC) framework. *Biol Psychiatry*. 2014; 76(5):350–353. [PubMed: 25103538]
2. Insel TR. Rethinking schizophrenia. *Nature*. 2010; 468(7321):187–193. [PubMed: 21068826]
3. Rapoport JL, Giedd JN, Gogtay N. Neurodevelopmental model of schizophrenia: update 2012. *Mol Psychiatry*. 2012; 17(12):1228–1238. [PubMed: 22488257]
4. Gur RE, Turetsky BI, Cowell PE, Finkelman C, Maany V, Grossman RI, et al. Temporolimbic volume reductions in schizophrenia. *Arch Gen Psychiatry*. 2000; 57(8):769–775. [PubMed: 10920465]
5. Bora E, Fornito A, Radua J, Walterfang M, Seal M, Wood SJ, et al. Neuroanatomical abnormalities in schizophrenia: a multimodal voxelwise meta-analysis and meta-regression analysis. *Schizophr Res*. 2011; 127(1):46–57. [PubMed: 21300524]
6. Selemon LD, Goldman-Rakic PS. The reduced neuropil hypothesis: a circuit based model of schizophrenia. *Biol Psychiatry*. 1999; 45(1):17–25. [PubMed: 9894571]
7. Laruelle M, Kegeles LS, Abi-Dargham A. Glutamate, dopamine, and schizophrenia. *Ann N Y Acad Sci*. 2006; 1003(1):138–158.
8. Poels EMP, Kegeles LS, Kantrowitz JT, Slifstein M, Javitt DC, Lieberman JA, et al. Imaging glutamate in schizophrenia: review of findings and implications for drug discovery. *Mol Psychiatry*. 2014; 19(1):20–29. [PubMed: 24166406]
9. Marsman A, van den Heuvel MP, Klomp DWJ, Kahn RS, Luijten PR, Pol HEH. Glutamate in schizophrenia: a focused review and meta-analysis of 1H-MRS studies. *Schizophr Bull*. 2013; 39(1):120–129. [PubMed: 21746807]
10. Remington G, Agid O, Foussias G. Schizophrenia as a disorder of too little dopamine: implications for symptoms and treatment. *Expert Rev Neurother*. 2011; 11(4):589–607. [PubMed: 21469931]
11. Lewis DA, Moghaddam B. Cognitive Dysfunction in Schizophrenia: Convergence of {gamma}-Aminobutyric Acid and Glutamate Alterations. *Arch Neurol*. 2006; 63(10):1372. [PubMed: 17030651]
12. Coyle JT. Glutamate and schizophrenia: beyond the dopamine hypothesis. *Cell Mol Neurobiol*. 2006; 26(4):363–382.
13. Moghaddam B. Targeting metabotropic glutamate receptors for treatment of the cognitive symptoms of schizophrenia. *Psychopharmacology (Berl)*. 2004; 174(1):39–44. [PubMed: 15205877]
14. Satterthwaite TD, Wolf DH, Calkins ME, Vandekar SN, Erus G, Ruparel K, et al. Structural brain abnormalities in youth with psychosis spectrum symptoms. *JAMA psychiatry*. 2016; 73(5):515–524. [PubMed: 26982085]
15. Egerton A, Stone JM, Chaddock CA, Barker GJ, Bonoldi I, Howard RM, et al. Relationship between brain glutamate levels and clinical outcome in individuals at ultra high risk of psychosis. *Neuropsychopharmacology*. 2014
16. Allen P, Chaddock CA, Egerton A, Howes OD, Barker G, Bonoldi I, et al. Functional outcome in people at high risk for psychosis predicted by thalamic glutamate levels and prefronto-striatal activation. *Schizophr Bull*. 2015; 41(2):429–439. [PubMed: 25123110]
17. Cannon TD, Cadenhead K, Cornblatt B, Woods SW, Addington J, Walker E, et al. Prediction of psychosis in youth at high clinical risk: a multisite longitudinal study in North America. *Arch Gen Psychiatry*. 2008; 65(1):28–37. [PubMed: 18180426]
18. Fusar-Poli P, Bonoldi I, Yung AR, Borgwardt S, Kempton MJ, Valmaggia L, et al. Predicting psychosis: meta-analysis of transition outcomes in individuals at high clinical risk. *Arch Gen Psychiatry*. 2012; 69(3):220. [PubMed: 22393215]
19. Merritt K, Egerton A, Kempton MJ, Taylor MJ, McGuire PK. Nature of Glutamate Alterations in Schizophrenia: A Meta-analysis of Proton Magnetic Resonance Spectroscopy Studies. *JAMA psychiatry*. 2016; 73(7):665–674. [PubMed: 27304221]
20. de la Fuente-Sandoval C, León-Ortiz P, Azcárraga M, Stephano S, Favila R, Díaz-Galvis L, et al. Glutamate levels in the associative striatum before and after 4 weeks of antipsychotic treatment in

- first-episode psychosis: a longitudinal proton magnetic resonance spectroscopy study. *JAMA psychiatry*. 2013; 70(10):1057–1066. [PubMed: 23966023]
21. Kegeles LS, Mao X, Stanford AD, Girgis R, Ojeil N, Xu X, et al. Elevated Prefrontal Cortex {gamma}-Aminobutyric Acid and Glutamate-Glutamine Levels in Schizophrenia Measured In Vivo With Proton Magnetic Resonance Spectroscopy. *Arch Gen Psychiatry*. 2012 archgenpsychiatry. 2011.1519 v2011.
  22. Wijtenburg S, Wright S, Korenic S, Gaston F, Ndubuizu N, Chiappelli J, et al. Altered Glutamate and Regional Cerebral Blood Flow Levels in Schizophrenia: A 1H-MRS and pCASL Study. *Neuropsychopharmacology: official publication of the American College of Neuropsychopharmacology*. 2016
  23. Theberge J, Bartha R, Drost DJ, Menon RS, Malla A, Takhar J, et al. Glutamate and glutamine measured with 4.0 T proton MRS in never-treated patients with schizophrenia and healthy volunteers. *Am J Psychiatry*. 2002; 159(11):1944–1946. [PubMed: 12411236]
  24. Beneyto M, Kristiansen LV, Oni-Orisan A, McCullumsmith RE, Meador-Woodruff JH. Abnormal glutamate receptor expression in the medial temporal lobe in schizophrenia and mood disorders. *Neuropsychopharmacology*. 2007; 32(9):1888–1902. [PubMed: 17299517]
  25. Goff DC, Coyle JT. The emerging role of glutamate in the pathophysiology and treatment of schizophrenia. *Am J Psychiatry*. 2001
  26. Tsai G, Coyle JT. Glutamatergic mechanisms in schizophrenia. *Annu Rev Pharmacol Toxicol*. 2002; 42(1):165–179. [PubMed: 11807169]
  27. Treen D, Battle S, Mollà L, Forcadell E, Chamorro J, Bulbena A, et al. Are there glutamate abnormalities in subjects at high risk mental state for psychosis? A review of the evidence. *Schizophr Res*. 2016
  28. Uhl I, Mavrogiorgou P, Norra C, Forstreuter F, Scheel M, Witthaus H, et al. 1H-MR spectroscopy in ultra-high risk and first episode stages of schizophrenia. *J Psychiatr Res*. 2011; 45(9):1135–1139. [PubMed: 21397254]
  29. Stone JM, Day F, Tsagaraki H, Valli I, McLean MA, Lythgoe DJ, et al. Glutamate dysfunction in people with prodromal symptoms of psychosis: relationship to gray matter volume. *Biol Psychiatry*. 2009; 66(6):533–539. [PubMed: 19559402]
  30. Keshavan MS, Dick RM, Diwadkar VA, Montrose DM, Prasad KM, Stanley JA. Striatal metabolic alterations in non-psychotic adolescent offspring at risk for schizophrenia: a 1 H spectroscopy study. *Schizophr Res*. 2009; 115(1):88–93. [PubMed: 19748228]
  31. Tibbo P, Hanstock C, Valiakalayil A, Allen P. 3-T proton MRS investigation of glutamate and glutamine in adolescents at high genetic risk for schizophrenia. *Am J Psychiatry*. 2004; 161(6):1116–1118. [PubMed: 15169703]
  32. Fusar-Poli P, Stone JM, Broome MR, Valli I, Mechelli A, McLean MA, et al. Thalamic glutamate levels as a predictor of cortical response during executive functioning in subjects at high risk for psychosis. *Arch Gen Psychiatry*. 2011; 68(9):881. [PubMed: 21536967]
  33. de la Fuente-Sandoval C, León-Ortiz P, Azcárraga M, Favila R, Stephano S, Graff-Guerrero A. Striatal glutamate and the conversion to psychosis: a prospective 1 H-MRS imaging study. *The International Journal of Neuropsychopharmacology*. 2013; 16(02):471–475. [PubMed: 22717289]
  34. de la Fuente-Sandoval C, Leon-Ortiz P, Favila R, Stephano S, Mamo D, Ramirez-Bermudez J, et al. Higher levels of glutamate in the associative-striatum of subjects with prodromal symptoms of schizophrenia and patients with first-episode psychosis. *Neuropsychopharmacology*. 2011; 36(9):1781–1791. [PubMed: 21508933]
  35. Tandon N, Bolo NR, Sanghavi K, Mathew IT, Francis AN, Stanley JA, et al. Brain metabolite alterations in young adults at familial high risk for schizophrenia using proton magnetic resonance spectroscopy. *Schizophr Res*. 2013
  36. Yoo SY, Yeon S, Choi C-H, Kang D-H, Lee J-M, Shin NY, et al. Proton magnetic resonance spectroscopy in subjects with high genetic risk of schizophrenia: investigation of anterior cingulate, dorsolateral prefrontal cortex and thalamus. *Schizophr Res*. 2009; 111(1):86–93. [PubMed: 19406622]

37. Purdon SE, Valiakalayil A, Hanstock CC, Seres P, Tibbo P. Elevated 3T proton MRS glutamate levels associated with poor Continuous Performance Test (CPT-0X) scores and genetic risk for schizophrenia. *Schizophr Res.* 2008; 99(1–3):218–224. [PubMed: 18248960]
38. Natsubori T, Inoue H, Abe O, Takano Y, Iwashiro N, Aoki Y, et al. Reduced frontal glutamate+glutamine and N-acetylaspartate levels in patients with chronic schizophrenia but not in those at clinical high risk for psychosis or with first-episode schizophrenia. *Schizophr Bull.* 2014; 40(5): 1128–1139. [PubMed: 24023251]
39. Schobel SA, Chaudhury NH, Khan UA, Paniagua B, Styner MA, Asllani I, et al. Imaging patients with psychosis and a mouse model establishes a spreading pattern of hippocampal dysfunction and implicates glutamate as a driver. *Neuron.* 2013; 78(1):81–93. [PubMed: 23583108]
40. Cai K, Haris M, Singh A, Kogan F, Greenberg JH, Hariharan H, et al. Magnetic resonance imaging of glutamate. *Nat Med.* 2012; 18(2):302–306. [PubMed: 22270722]
41. Cai K, Singh A, Roalf DR, Nanga RPR, Haris M, Hariharan H, et al. Mapping glutamate in subcortical brain structures using high-resolution GluCEST MRI. *NMR Biomed.* 2013
42. Kogan F, Singh A, Debrosse C, Haris M, Cai K, Nanga RP, et al. Imaging of glutamate in the spinal cord using GluCEST. *Neuroimage.* 2013; 77:262–267. [PubMed: 23583425]
43. van Zijl P, Yadav NN. Chemical exchange saturation transfer (CEST): what is in a name and what isn't? *Magn Reson Med.* 2011; 65(4):927–948. [PubMed: 21337419]
44. Sherry AD, Woods M. Chemical exchange saturation transfer contrast agents for magnetic resonance imaging. *Annual review of biomedical engineering.* 2008; 10:391.
45. Zhou J, van Zijl PC. Chemical exchange saturation transfer imaging and spectroscopy. *Progress in Nuclear Magnetic Resonance Spectroscopy.* 2006; 48(2):109–136.
46. Henkelman R, Stanisz G, Graham S. Magnetization transfer in MRI: a review. *NMR Biomed.* 2001; 14(2):57–64. [PubMed: 11320533]
47. Haris M, Nath K, Cai K, Singh A, Crescenzi R, Kogan F, et al. Imaging of glutamate neurotransmitter alterations in Alzheimer's disease. *NMR Biomed.* 2013; 26(4):386–391. [PubMed: 23045158]
48. Crescenzi R, DeBrosse C, Nanga RPR, Reddy S, Haris M, Hariharan H, et al. In vivo measurement of glutamate loss is associated with synapse loss in a mouse model of tauopathy. *Neuroimage.* 2014; 101:185–192. [PubMed: 25003815]
49. Pépin J, Francelle L, Carrillo-de Sauvage M-A, de Longprez L, Gipchtein P, Cambon K, et al. In vivo imaging of brain glutamate defects in a knock-in mouse model of Huntington's disease. *Neuroimage.* 2016; 139:53–64. [PubMed: 27318215]
50. Davis KA, Nanga RPR, Das S, Chen SH, Hadar PN, Pollard JR, et al. Glutamate imaging (GluCEST) lateralizes epileptic foci in nonlesional temporal lobe epilepsy. *Sci Transl Med.* 2015; 7(309):309ra161–309ra161.
51. Kaufman J, Birmaher B, Brent D, Rao U, Flynn C, Moreci P, et al. Schedule for Affective Disorders and Schizophrenia for School-Age Children-Present and Lifetime Version (K-SADS-PL): initial reliability and validity data. *J Am Acad Child Adolesc Psychiatry.* 1997; 36(7):980–988. [PubMed: 9204677]
52. First, MB., Spitzer, RL., Gibbon, M., Williams, JBW. Structured Clinical Interview for DSM-IV-TR Axis I Disorders, Research Version, Patient Edition (SCID-I/P). Biometrics Research, New York State Psychiatric Institute; New York: 2002.
53. McGlashan TH, Miller TJ, Woods SW, Hoffman RE, Davidson L. Instrument for the assessment of prodromal symptoms and states. *Early intervention in psychotic disorders.* 2001:135–149.
54. Overall JE, Gorham DR. The brief psychiatric rating scale. *Psychol Rep.* 1962; 10:799–812.
55. Andreasen, NC. The Scale for the Assessment of Negative Symptoms (SANS). Iowa City, Iowa: University of Iowa; 1984.
56. Andreasen, NC. The Scale for the Assessment of Positive Symptoms (SAPS). Iowa City, Iowa: University of Iowa; 1984.
57. Miller TJ, McGlashan TH, Woods SW, Stein K, Driesen N, Corcoran CM, et al. Symptom assessment in schizophrenic prodromal states. *Psychiatr Q.* 1999; 70(4):273–287. [PubMed: 10587984]

58. Roalf DR, Quarmley M, Elliott MA, Satterthwaite TD, Vandekar SN, Ruparel K, et al. The impact of quality assurance assessment on diffusion tensor imaging outcomes in a large-scale population-based cohort. *Neuroimage*. 2016; 125:903–919. [PubMed: 26520775]
59. Gur RE, Turetsky BI, Bilker WB, Gur RC. Reduced gray matter volume in schizophrenia. *Arch Gen Psychiatry*. 1999; 56(10):905. [PubMed: 10530632]
60. Karlsgodt KH, Niendam TA, Bearden CE, Cannon TD. White matter integrity and prediction of social and role functioning in subjects at ultra-high risk for psychosis. *Biol Psychiatry*. 2009; 66(6):562–569. [PubMed: 19423081]
61. Roalf DR, Gur RE, Verma R, Parker WA, Quarmley M, Ruparel K, et al. White matter microstructure in schizophrenia: Associations to neurocognition and clinical symptomatology. *Schizophr Res*. 2015; 161(1):42–49. [PubMed: 25445621]
62. Provencher SW. Estimation of metabolite concentrations from localized in vivo proton NMR spectra. *Magn Reson Med*. 1993; 30(6):672–679. [PubMed: 8139448]
63. Brugger S, Davis JM, Leucht S, Stone JM. Proton magnetic resonance spectroscopy and illness stage in schizophrenia: a systematic review and meta-analysis. *Biol Psychiatry*. 2011; 69(5):495–503. [PubMed: 21145039]
64. Falkenberg LE, Westerhausen R, Specht K, Hugdahl K. Resting-state glutamate level in the anterior cingulate predicts blood-oxygen level-dependent response to cognitive control. *Proc Natl Acad Sci U S A*. 2012; 109(13):5069–5073. [PubMed: 22411802]
65. Stanley JA, Vemulapalli M, Nutche J, Montrose DM, Sweeney JA, Pettegrew JW, et al. Reduced N-acetyl-aspartate levels in schizophrenia patients with a younger onset age: A single-voxel 1H spectroscopy study. *Schizophr Res*. 2007; 93(1):23–32. [PubMed: 17498928]
66. Tebartz van Elst L, Valerius G, Buchert M, Thiel T, Rusch N, Bubl E, et al. Increased prefrontal and hippocampal glutamate concentration in schizophrenia: evidence from a magnetic resonance spectroscopy study. *Biol Psychiatry*. 2005; 58(9):724–730. [PubMed: 16018980]
67. Theberge J, Al-Semaan Y, Williamson PC, Menon RS, Neufeld RWJ, Rajakumar N, et al. Glutamate and glutamine in the anterior cingulate and thalamus of medicated patients with chronic schizophrenia and healthy comparison subjects measured with 4. 0-T proton MRS. *Am J Psychiatry*. 2003; 160(12):2231–2233. [PubMed: 14638596]
68. Olney JW, Farber NB. Glutamate receptor dysfunction and schizophrenia. *Arch Gen Psychiatry*. 1995
69. van Erp TGM, Hibar DP, Rasmussen JM, Glahn DC, Pearlson GD, Andreassen OA, et al. Subcortical brain volume abnormalities in 2028 individuals with schizophrenia and 2540 healthy controls via the ENIGMA consortium. *Mol Psychiatry*. 2015
70. Roalf DR, Vandekar SN, Almasy L, Ruparel K, Satterthwaite TD, Elliott MA, et al. Heritability of subcortical and limbic brain volume and shape in multiplex-multigenerational families with schizophrenia. *Biol Psychiatry*. 2015; 77(2):137–146. [PubMed: 24976379]
71. Glahn DC, Laird AR, Ellison-Wright I, Thelen SM, Robinson JL, Lancaster JL, et al. Meta-analysis of gray matter anomalies in schizophrenia: application of anatomic likelihood estimation and network analysis. *Biol Psychiatry*. 2008; 64(9):774–781. [PubMed: 18486104]
72. Gur RE, Maany V, Mozley PD, Swanson C, Bilker W, Gur RC. Subcortical MRI volumes in neuroleptic-naive and treated patients with schizophrenia. *Am J Psychiatry*. 1998; 155(12):1711–1717. [PubMed: 9842780]
73. Moghaddam B, Javitt D. From revolution to evolution: the glutamate hypothesis of schizophrenia and its implication for treatment. *Neuropsychopharmacology*. 2012; 37(1):4–15. [PubMed: 21956446]
74. Liddle P, Friston K, Frith C, Hirsch S, Jones T, Frackowiak R. Patterns of cerebral blood flow in schizophrenia. *Br J Psychiatry*. 1992; 160(2):179–186. [PubMed: 1540757]
75. Goghari VM, Sponheim SR, MacDonald AW. The functional neuroanatomy of symptom dimensions in schizophrenia: a qualitative and quantitative review of a persistent question. *Neurosci Biobehav Rev*. 2010; 34(3):468–486. [PubMed: 19772872]
76. Ford JM, Roach BJ, Faustman WO, Mathalon DH. Synch before you speak: auditory hallucinations in schizophrenia. *Am J Psychiatry*. 2007; 164(3):458–466. [PubMed: 17329471]

77. Stone J, Kotoula V, Dietrich C, De Simoni S, Krystal JH, Mehta MA. Perceptual distortions and delusional thinking following ketamine administration are related to increased pharmacological MRI signal changes in the parietal lobe. *Journal of Psychopharmacology*. 2015; 29(9):1025–1028. [PubMed: 26152321]
78. Stone JM, Dietrich C, Edden R, Mehta MA, De Simoni S, Reed LJ, et al. Ketamine effects on brain GABA and glutamate levels with 1H-MRS: relationship to ketamine-induced psychopathology. *Mol Psychiatry*. 2012; 17(7)

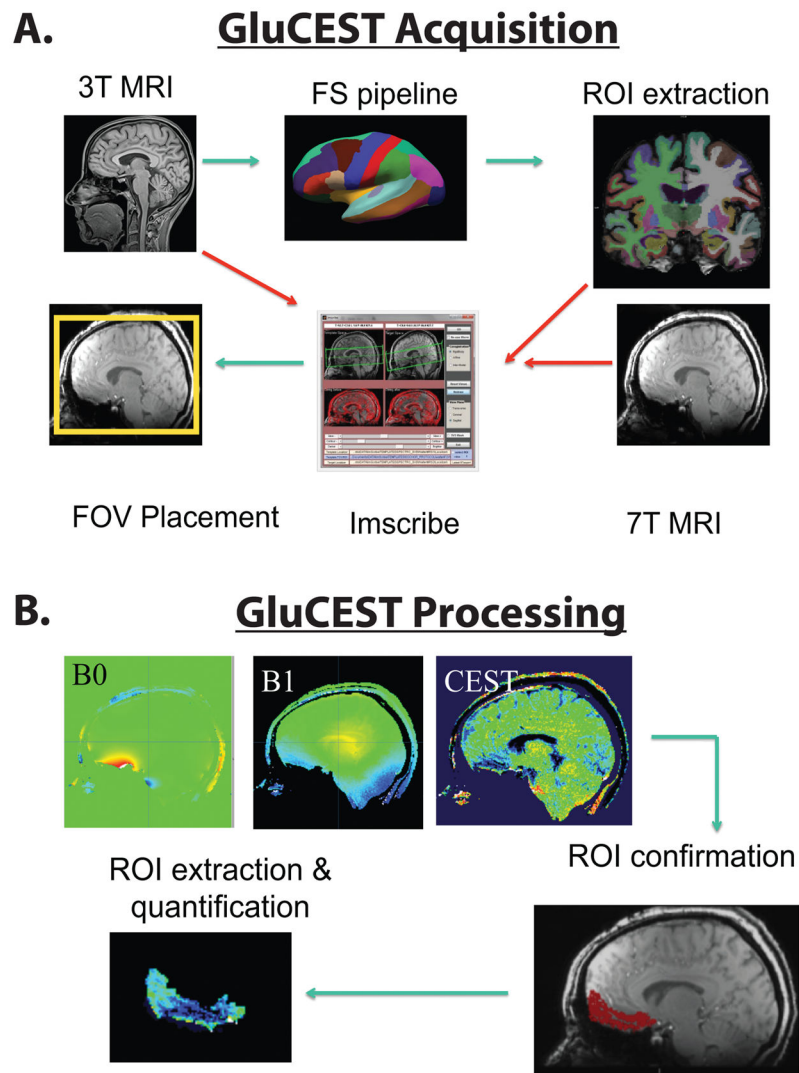


**Figure 1.** Schematic representation of the data acquisition and analysis. An optimized within-subject acquisition and analysis pipeline was implemented. Participants underwent both 3T and 7T MRI. At 3T, structural images were acquired and each subject's image was segmented using FreeSurfer. Regions of interest were extracted, registered in real-time to each participant's 7T structural scan via Imscribe. This information was then used to place the acquisition field of view for 7T GluCEST. At 7T, single slice GluCEST,  $B_0$  and  $B_1$  maps (5mm thickness) were collected in mid-sagittal planes. Placement of the ROIs was validated in offline analysis by extracting and registering a corresponding 5mm slab from the whole-brain MPRAGE to the GluCEST acquisition volume to confirm voxel placement. GluCEST contrast (%) was then extracted from regions of interest and tabulated off-line.

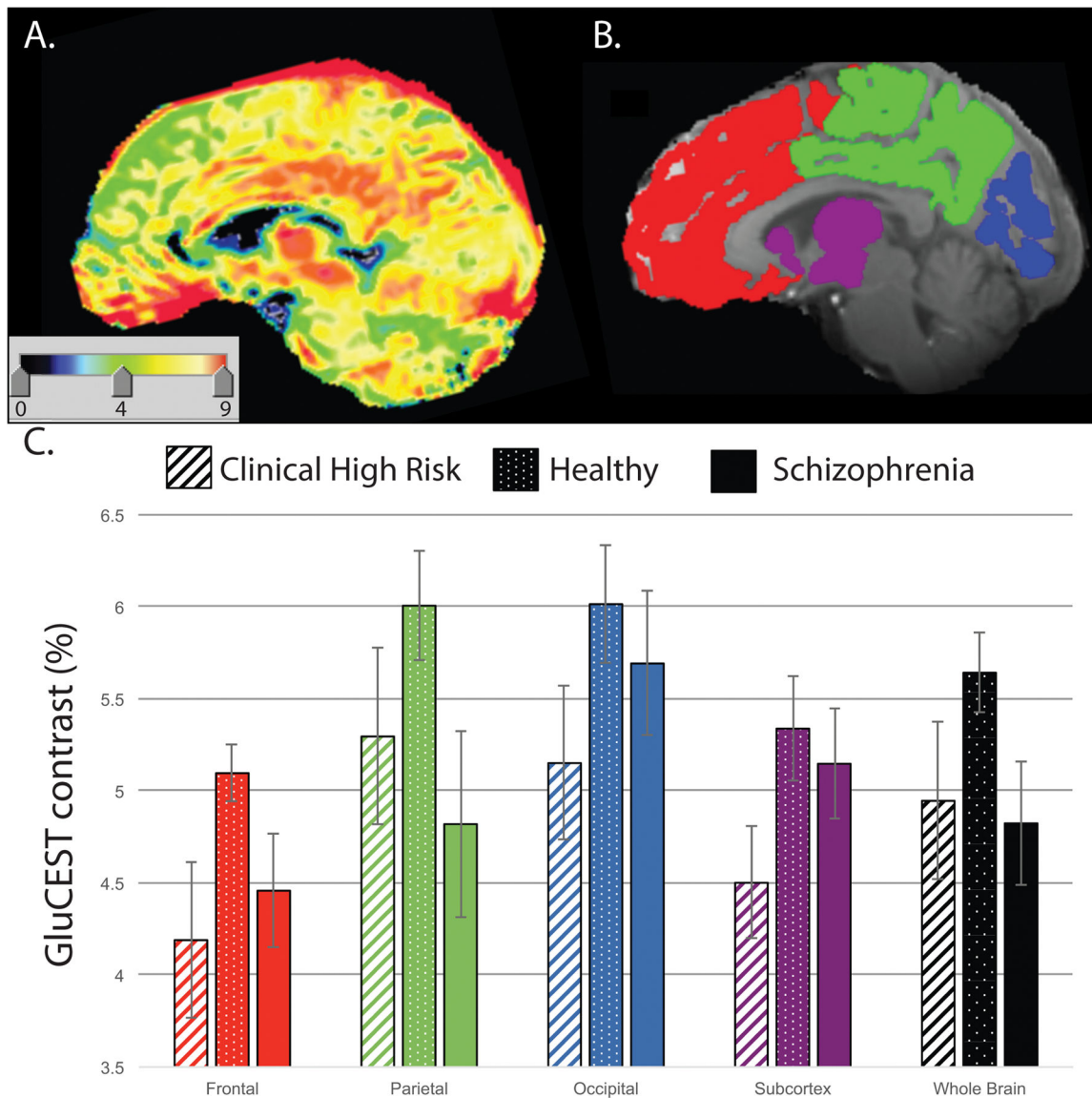


**Figure 2.**

**A:** An example single slice GluCEST map. **B:** Lobar ROIs used for GluCEST data extraction. **C:** Mean whole slice, subcortical and lobar GluCEST contrast (%) measures ( $\pm$  s.e.m.) in healthy individuals, clinical high risk subjects and schizophrenia patients. GluCEST contrast was significantly lower, across the subcortex and three cortical lobes, in the psychosis spectrum sample as a whole and in the clinical high risk sample alone, when compared to control subjects.

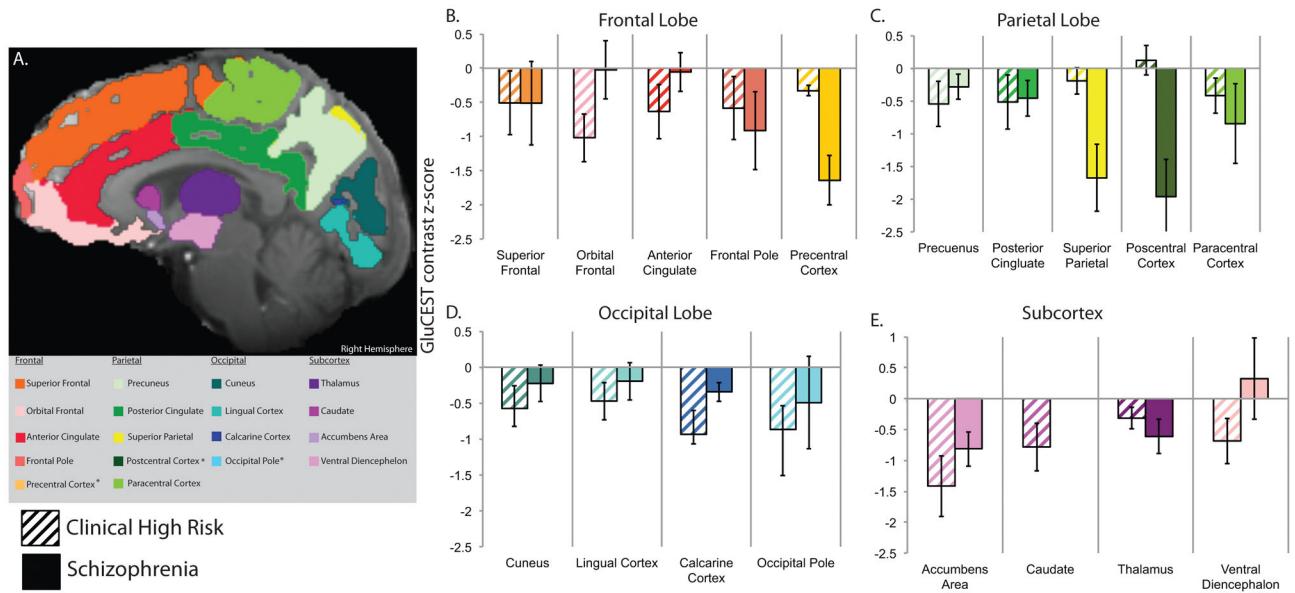


**Figure 3.** **A.** Region of interest labels used for GluCEST data extraction. **B.** Z-scores (mean  $\pm$  s.e.m.) for GluCEST contrast in each region of interest in the frontal (B), parietal (C) and occipital (D) cortices and subcortex (E). Scores for schizophrenia patients and clinical high risk subjects are scaled relative to healthy controls who have standardized Z-scores of mean=0 and standard deviation=1. Note: No normalized GluCEST data was available within the caudate for patients with SZ as only one patient had viable data within this region.

**Table 1**

## Participant Characteristics

	Healthy Controls	Psychosis Spectrum	
	HC (n=17)	CHR (n=14)	SZ (n=5)
Sex (n)			
Male	8	8	4
Female	9	6	1
Race (n)			
Black	6	8	1
White	9	3	2
Mixed/Other	2	3	2
Age (Mean $\pm$ SD)	19.6 $\pm$ 2.5	18.4 $\pm$ 2.7	21.8 $\pm$ 2.5
Maternal Education	15.2 $\pm$ 2.1	14.6 $\pm$ 2.3	14.6 $\pm$ 3.4
SOPS Ratings			
Positive	0.6 $\pm$ 2.0	8.5 $\pm$ 5.5	21.6 $\pm$ 5.1
Negative	0.6 $\pm$ 1.4	7.4 $\pm$ 4.7	16.4 $\pm$ 5.3
Disorganized	0.5 $\pm$ 1.0	2.9 $\pm$ 2.7	9.0 $\pm$ 7.6
General	0.5 $\pm$ 0.9	3.1 $\pm$ 3.2	6.0 $\pm$ 3.3
SANS Total Score	1.9 $\pm$ 6.3	18.9 $\pm$ 17.1	32.2 $\pm$ 18.6
SAPS Total Score	0 $\pm$ 0	10.5 $\pm$ 9.4	33.8 $\pm$ 15.0
GAF Score	83.8 $\pm$ 8.2	60.1 $\pm$ 10.6	46.4 $\pm$ 6.8
Illness Duration (yrs)	N/A	N/A	2.6 $\pm$ 1.1
Current Medication (n)			
Antipsychotics	0	0	3
Antidepressants	0	0	2

**Table 2**

Regional GluCEST contrast (%) values by clinical condition.

GluCEST Contrast (%) Mean (SEM)	Healthy Controls		Psychosis Spectrum		% With GluCEST
	HC (n=17)	CHR (n=14)	SZ (n=5)		
Whole Slice Cortex	5.64 (0.22)	4.95 (0.43)	4.82 (0.33)		100
Frontal Lobe	5.10 (0.15)	4.19 (0.42)	4.46 (0.31)		100
Superior Frontal	5.04 (0.23)	4.56 (0.44)	4.56 (0.58)		100
Orbital Frontal	5.52 (0.32)	4.18 (0.46)	5.48 (0.56)		100
Anterior Cingulate	5.20 (0.30)	4.41 (0.50)	5.12 (0.35)		100
Frontal Pole	4.30 (0.31)	3.58 (0.57)	3.18 (0.70)		97
Precentral Cortex	5.32 (0.35)	4.97 (0.21)	3.60 (0.60)		36
Parietal Lobe	6.01 (0.30)	5.30 (0.48)	4.82 (0.51)		100
Precuneus	6.24 (0.35)	5.46 (0.50)	5.84 (0.31)		97
Posterior Cingulate	6.52 (0.28)	5.92 (0.48)	5.99 (0.32)		100
Superior Parietal	6.03 (0.33)	5.78 (0.37)	3.84 (0.86)		72
Postcentral Cortex	5.19 (0.36)	5.34 (0.43)	2.76 (0.92)		58
Paracentral Cortex	6.09 (0.60)	5.08 (0.70)	4.04 (1.90)		86
Occipital Lobe	6.01 (0.33)	5.15 (0.43)	5.69 (0.39)		94
Cuneus	6.07 (0.31)	5.36 (0.40)	5.79 (0.31)		94
Lingual Cortex	5.81 (0.35)	5.16 (0.37)	5.54 (0.36)		94
Calcarine Cortex	5.83 (0.36)	4.49 (0.42)	5.34 (0.21)		83
Occipital Pole	6.36 (0.47)	4.83 (0.68)	5.49 (1.46)		75
Subcortex	5.41 (0.35)	4.46 (0.47)	5.12 (0.43)		100
Accumbens Area	6.68 (0.33)	5.09 (0.66)	5.69 (0.29)		86
Caudate	4.14 (0.35)	3.17 (0.48)	4.53 (-) <sup>#</sup>		61
Thalamus	5.38 (0.40)	5.00 (0.27)	4.67 (0.37)		100
Ventral Diencephalon	5.42 (0.31)	4.57 (0.45)	5.58 (0.62)		94

% with GluCEST = the percentage of individuals with usable data from a region-of-interest.

<sup>#</sup>Only one patient with SZ provided values.